

DESY 04-041  
SFB/PPP-04-08  
March 2004

## Finite size effects of a pion matrix element

M. Guagnelli<sup>a</sup>, K. Jansen<sup>b</sup>, F. Palombi<sup>a,c</sup>,  
R. Petronzio<sup>a</sup>, A. Shindler<sup>b</sup> and I. Wetzorke<sup>b</sup>

Zeuthen-Rome (ZeRo) Collaboration

<sup>a</sup> Dipartimento di Fisica, Università di Roma *Tor Vergata*  
and INFN, Sezione di Roma II,

Via della Ricerca Scientifica 1, I-00133 Rome, Italy

<sup>b</sup> NIC/DESY Zeuthen, Platanenallee 6, D-15738 Zeuthen, Germany

<sup>c</sup> *E. Fermi* Research Center, c/o Compendio Viminale, pal. F, I-00184 Rome, Italy

### Abstract

We investigate finite size effects of the pion matrix element of the non-singlet, twist-2 operator corresponding to the average momentum of non-singlet quark densities. Using the quenched approximation, they come out to be surprisingly large when compared to the finite size effects of the pion mass. As a consequence, simulations of corresponding nucleon matrix elements could be affected by finite size effects even stronger which could lead to serious systematic uncertainties in their evaluation.

# 1 Introduction

A complete description of moments of parton distribution functions (PDF) from first principles is still missing. In order to provide reliable numerical determinations, it is necessary to control all systematic uncertainties which include the continuum limit, non-perturbative renormalization, chiral extrapolation, finite size effects and quenching. Several studies on hadron matrix elements of twist-2 operators have been performed since now [1, 2]. In [2] a study of the continuum limit employing a perturbative renormalization shows small cutoff effects. Applying a non-perturbative renormalization [3], slightly reduces an observed discrepancy between theory and experiment [4]. First computations in the unquenched case [1], at a rather high value of the quark mass, seems to indicate no quantitative differences with the quenched case. In [5] it has been suggested that the discrepancy between theory and experiment could be explained by a rather strong dependence of the matrix elements on the quark mass in the chiral region when a very small quark mass is entered. The simulations performed since now are carried out at values of the quark mass too far away from the physical point to test this anticipated mass dependence. One problem that to our knowledge has not been faced in a systematic manner is how the finite size of the lattice can influence such computations.

In this letter we present a study of the finite size effects (FSE) of the quenched pion matrix element of the twist-2 operator corresponding to the average momentum of non-singlet quark densities. Preliminary results were presented at the last lattice conference [6].

It has already been noticed some time ago [7] and more recently in [8, 9], that FSE especially in the unquenched case can be a serious source of systematic error. In this letter we want to emphasize that even in the quenched case, FSE for pion 3-point functions involving twist-2 operators, can be much larger than the FSE for the hadron masses. Thus, there is a clear warning that for the unquenched case and moreover for nucleon matrix elements such FSE should be studied very carefully in order to avoid an underestimation of this systematic effect.

## 2 Setup and basic definitions

The moments of parton distribution functions (PDF)  $\langle x^{(N-1)} \rangle$  are related to matrix elements of leading twist  $\tau$  ( $\tau = \text{dim-spin}$ ) operators  $\mathcal{O}$  of given spin, between hadron states  $h(p)$

$$\begin{aligned} \langle h(p) | \mathcal{O}_{\mu_1 \dots \mu_N} | h(p) \rangle &= M^{(N-1)}(\mu) p_{\mu_1} \cdots p_{\mu_n} \\ &+ \text{terms } \delta_{\mu_i \mu_j} \end{aligned} \quad (1)$$

$$\langle x^{(N-1)} \rangle(\mu) = M^{(N-1)}(\mu = Q) , \quad (2)$$

where the renormalization scale  $\mu$  is identified with the momentum transfer  $Q$  in deep inelastic scattering (DIS).

Our setup of lattice QCD is on a hyper-cubic euclidean lattice with spacing  $a$  and size  $L^3 \times T$ . We impose periodic boundary conditions in the spatial directions and Dirichlet boundary conditions in time, as they are used to formulate the Schrödinger functional (SF) [10] (we refer to these references for unexplained notations). In this paper we will consider homogeneous boundary conditions, where the spatial components of the gauge potentials at the boundaries and also the fermion boundary source fields are set to zero. In this case the Schrödinger functional partition function can be written as [11]

$$\mathcal{Z} = \langle i_0 | e^{-T\mathbb{H}} \mathbb{P} | i_0 \rangle \quad (3)$$

where the initial and final states  $|i_0\rangle$  carry the quantum numbers of the vacuum. We have studied the matrix elements between charged pion states of the following operator

$$\mathcal{O}_{44}(x) = \frac{1}{2} \bar{\psi}(x) \left[ \gamma_4 \overleftrightarrow{D}_4 - \frac{1}{3} \sum_{k=1}^3 \gamma_k \overleftrightarrow{D}_k \right] \psi(x) . \quad (4)$$

We indicate with  $\zeta$  and  $\bar{\zeta}$  (and the corresponding  $\zeta'$  and  $\bar{\zeta}'$ ) a flavour doublet. As discussed in [12] we recall that  $\zeta$ ,  $\bar{\zeta}$ ,  $\zeta'$  and  $\bar{\zeta}'$  are functional derivatives with respect to the boundary source fields.

The states with charged pion quantum numbers in the Schrödinger functional are the dimensionless fields

$$\mathbb{S} = \frac{a^6}{L^3} \sum_{\mathbf{y}, \mathbf{z}} \bar{\zeta}(\mathbf{y}) \gamma_5 \tau^+ \zeta(\mathbf{z}) \quad \mathbb{S}' = \frac{a^6}{L^3} \sum_{\mathbf{u}, \mathbf{v}} \bar{\zeta}'(\mathbf{u}) \gamma_5 \tau^- \zeta'(\mathbf{v}) \quad (5)$$

where  $\tau^\pm = \frac{1}{\sqrt{2}}(\tau^1 \pm i\tau^2)$  and  $\tau^k$  with  $k = 1, 2, 3$  are the usual Pauli matrices. The correlation function to extract the matrix element is

$$f_{44}(x_0) = \langle \mathbb{S} \mathcal{O}_{44}(x) \mathbb{S}' \rangle . \quad (6)$$

The Wick contractions of this correlation function contain also a disconnected piece that we neglect consistently with the fact that we will do quenched simulations. For normalization purposes it is important to define

$$f_1 = -\frac{1}{2} \langle \mathbb{S} \mathbb{S}' \rangle . \quad (7)$$

The correlation functions  $f_{44}$  and  $f_1$  have the following quantum mechanical representations

$$f_{44}(x_0) = \mathcal{Z}^{-1} \langle i_\pi | e^{-(T-x_0)\mathbb{H}} \mathbb{P} \mathcal{O}_{44}(x) e^{-x_0\mathbb{H}} \mathbb{P} | i_\pi \rangle \quad (8)$$

$$f_1 = \mathcal{Z}^{-1} \frac{1}{2} \langle i_\pi | e^{-T\mathbb{H}} \mathbb{P} | i_\pi \rangle . \quad (9)$$

Inserting a complete set of eigenstates of the Hamiltonian and retaining only the first non-leading corrections we have

$$f_{44}(x_0) \simeq \rho^2 \langle 0, \pi | \mathcal{O}_{44}(x) | 0, \pi \rangle e^{-m_\pi T} \{1 + \eta_{\mathcal{O}_{44}}^\pi e^{-x_0 \Delta} + \eta_{\mathcal{O}_{44}}^\pi e^{-(T-x_0)\Delta}\} \quad (10)$$

$$f_1 \simeq \rho^2 e^{-m_\pi T} . \quad (11)$$

The matrix element we are interested in, neglecting contributions from excited states, can then be extracted from the plateau value of the following ratio:

$$\frac{f_{44}(x_0)}{f_1} = \langle 0, \pi | \mathcal{O}_{44}(x) | 0, \pi \rangle . \quad (12)$$

In order to relate this numerically computed ratio with the corresponding continuum operators in the Minkowski space, we need a suitable normalization factor

$$\langle x \rangle = \frac{2\kappa}{m_\pi} \langle 0, \pi | \mathcal{O}_{44}(x) | 0, \pi \rangle , \quad (13)$$

where we always take for  $m_\pi$  the infinite volume pion mass  $m_\pi(L = \infty)$ , summarized in table 2, in order to disentangle the FSE of the pion mass and  $\langle x \rangle$  itself. Furthermore, we consider only the bare matrix elements without renormalization factor, since the FSE remain unchanged when employing the appropriate  $Z$  factors.

Using the procedure of ref. [11] we have extracted the plateau values for the effective pion mass and the 3-point function with a systematic relative error coming from the excited states of 0.1%, respectively 0.4%, well below the statistical accuracy of our computations. Technical details can be found in a forthcoming publication [13].

### 3 Numerical details and results

We have performed a set of quenched simulations at fixed lattice spacing  $a = 0.079$  fm ( $\beta = 6.1$ ), for three values of the quark mass ( $\kappa = 0.1340, 0.1345, 0.1350$ ), and several lattice sizes, using the non-perturbatively improved clover action [14]. For some simulations we have also used two different time extents of our lattice ( $T, T'$ , with  $T' < T$ ). Our simulation parameters are summarized in table 1. Using  $r_0 = 0.5$  fm to fix the scale [15], we have lattice sizes varying between 0.9 fm and 2.5 fm, and values of  $z = m_\pi L$  varying between 2.5 and 11.2.

We have made fits of the data both with an exponential and power dependence on the lattice size  $L$  (in the following equation we generically indicate with  $F(L)$  both  $m_\pi$  and  $\langle x \rangle$ ):

$$\text{exp :} \quad F(L) = a_0 + \frac{a_1}{L^{3/2}} \exp\{-a_2 L\} \quad (14)$$

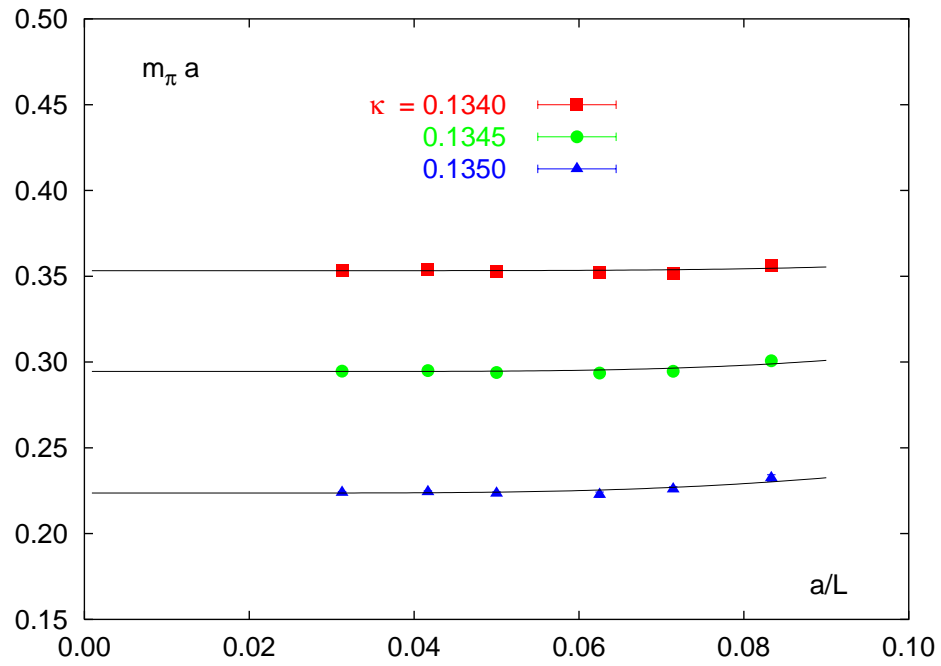


Figure 1: Finite size dependence of the pion mass for three values of the quark masses. The curves show the exponential fit of eq. (14) with  $a_2 = m_\pi$  fixed (see text).

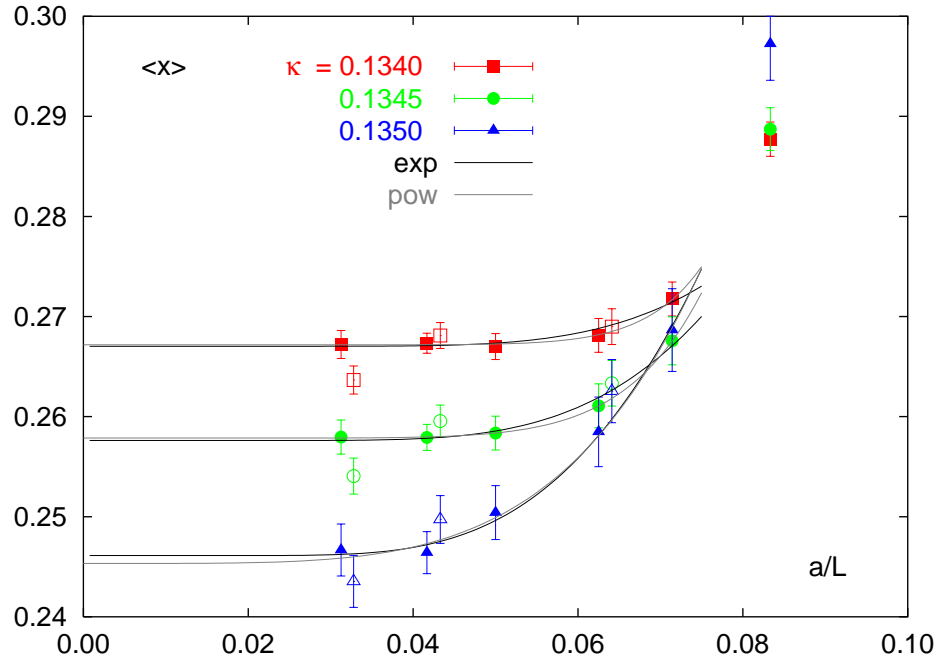


Figure 2: Finite size dependence of the twist-2 operator matrix element for three values of the quark masses. The curves show both the exponential ( $a_2 = m_\pi$  fixed) and the power law fits (see text). The open symbols denote simulation results with lattices of the same spatial extent, but with a shorter time extent (see text). They are slightly displaced in  $a/L$  for better visibility.

$L/a$	$T/a$	$N$
12	36	3200
14	36	1600
16	36	800
16	42	800
24	36	800
24	42	800
32	36	400
32	56	185

Table 1: Parameters of our simulation points.  $N$  denotes the number of measurements taken into account.

	$m_\pi(L = \infty)$	$\chi^2/dof$	$\langle x \rangle(L = \infty)$	$\chi^2/dof$
exp: $\kappa = 0.1340$	0.3533(3)	1.7	0.2672(7)	0.03
0.1345	0.2946(3)	0.6	0.2579(10)	0.002
0.1350	0.2239(4)	0.6	0.2458(24)	0.12
exp*: $\kappa = 0.1340$	0.3533(3)	2.2	0.2670(7)	0.12
0.1345	0.2945(3)	2.0	0.2576(9)	0.08
0.1350	0.2237(4)	1.6	0.2461(15)	0.09
pow: $\kappa = 0.1340$	0.3533(3)	1.6	0.2671(6)	0.03
0.1345	0.2946(3)	0.6	0.2579(11)	0.002
0.1350	0.2239(4)	0.6	0.2453(29)	0.17

Table 2: Results for the infinite volume limit of  $m_\pi$  and  $\langle x \rangle$  using the exponential fit (exp) of eq. (14), fixing  $a_2 = m_\pi$  (exp\*) and employing the power law fit of eq. (15) to describe the FSE.

$$\text{pow : } \quad F(L) = a_0 + a_1/L^{a_2} \quad (15)$$

The values of  $m_\pi(L = \infty)$  as obtained from the different fits are summarized in table 2 complemented by  $\chi^2/dof$ . In fig. 1 we show the size dependence of  $m_\pi$  for the three quark masses. The solid curves show the exponential fits keeping  $a_2 = m_\pi$  fixed. Also a power law fit describes the data rather well and leads to a comparable number of the infinite volume pion mass. For the pion mass in the unquenched case it is inferred that for very small lattices the FSE are described by a power law behaviour [16]. In this case the source of the FSE is the squeezing of the hadron in a small volume. Before the asymptotic (infinite volume) region is reached, there is a pre-asymptotic region where the unquenched FSE are described by an exponential law [17] indicating that the source of the FSE is the wrapping around the world of the virtual pions. Our data obtained in the quenched approximation can not differentiate between these two cases.

In fig. 2 we show the finite size dependence of  $\langle x \rangle$  for the three quark masses. As expected, the FSE turn out to be stronger for lighter quark masses when keeping

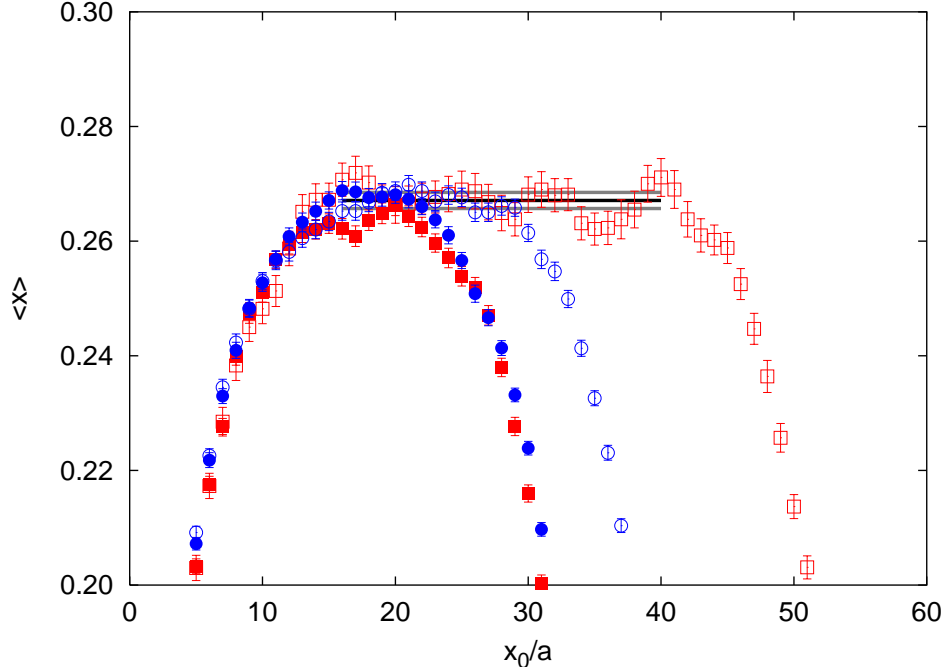


Figure 3: Time dependence of the 3-point function for  $\kappa = 0.1340$  coming from the following lattice sizes:  $32^3 \times 56$ ,  $32^3 \times 36$  (squares),  $24^3 \times 42$  and  $24^3 \times 36$  (circles).

the box size fixed. At present there are no predictions of the form of the FSE for a matrix element such as  $\langle x \rangle$ . As an ansatz, we have used the same fit functions as for the pion mass. Again, the comparison of the matrix element with both fit functions does not allow to prefer either of the two fit functions. Thus, carrying over the previous arguments for the pion mass to the 3-point function, it is difficult to disentangle which is the physical origin of the FSE of the matrix element.

At this point we want to make a short remark about the importance of the physical extent of the plateau in time direction. In fig. 2 the empty symbols show the values of  $\langle x \rangle$  obtained with lattices of the same spatial extent, but with a shorter time extent ( $T' \sim 2.8 \text{ fm} < T \sim 3.3 - 4.4 \text{ fm}$ ). Comparing  $\langle x \rangle$  on the lattices  $L/a = 24$  and  $L/a = 32$  with smaller time extent, it looks like there would still be some FSE. This is, however, not the case and the explanation of this effect has a different source. Since it takes around 1.3 fm before all the contributions of the excited states go below the accuracy of our computation, a time extent below or around 3 fm can be a source of an in-accurate determination of the plateau value, given the small number of points available. In fig. 3 we plot the time dependence of the 3-point function for  $\kappa = 0.1340$ , coming from lattices with different spatial extents ( $L/a = 24, 32$ ) and different time extents ( $T/a = 36, 42, 56$ ). The two spatial extents should be large enough, for all our quark masses, to be free from FSE. Since the contributions of the excited states have already died out at around 1.3 fm, even if the plateau is short it should give results consistent with the result obtained from a longer time extent. From fig. 3 it is clear that the disagreement between the two



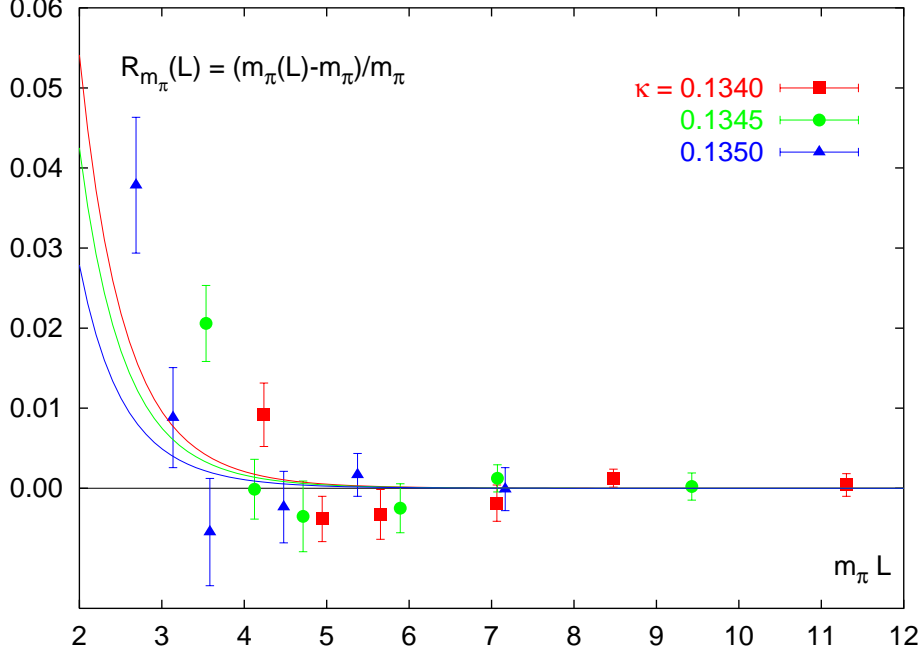


Figure 4: Finite size dependence of  $m_\pi$  as a function of  $z = m_\pi L$ . The solid curves show the FSE for the pion mass described by formula (17).

time extents is given by a statistical fluctuation that plays the role of a systematic error due to the short time extent. In the longer time extent case too, there is a wiggling in the plateau due to statistical fluctuations, but in the short time extent case the plateau is not long enough to average away these statistical fluctuations. This is also consistent with the fact that for the two different spatial sizes this fluctuation goes in opposite directions. A warning we want to give is that if the number of points in the plateau is only around 3 – 5 there is the risk to have results biased by 2 – 3  $\sigma$ , that obviously are consistent with being a statistical fluctuation.

It is however quite clear that the FSE for the 3-point functions are much larger than for the pion mass. In order to make this statement more quantitative we have plotted the relative systematic deviation

$$R_F(L) = \frac{F(L) - F(L = \infty)}{F(L = \infty)} \quad F(L) = m_\pi(L), \langle x \rangle(L) \quad (16)$$

as functions of  $m_\pi L$ , where  $m_\pi$  is the infinite volume pion mass. Since the FSE for the pion mass are very small, it makes no difference to study the dependence of the data as functions of  $m_\pi(L)L$  or  $m_\pi(L = \infty)L$ . In fig. 4 and 5 we see that both the data sets scale in a good way as function of  $m_\pi L$ . Apart from the  $L/a = 12$  points the data sets are in agreement with the formula given in ref. [19, 20] to leading order

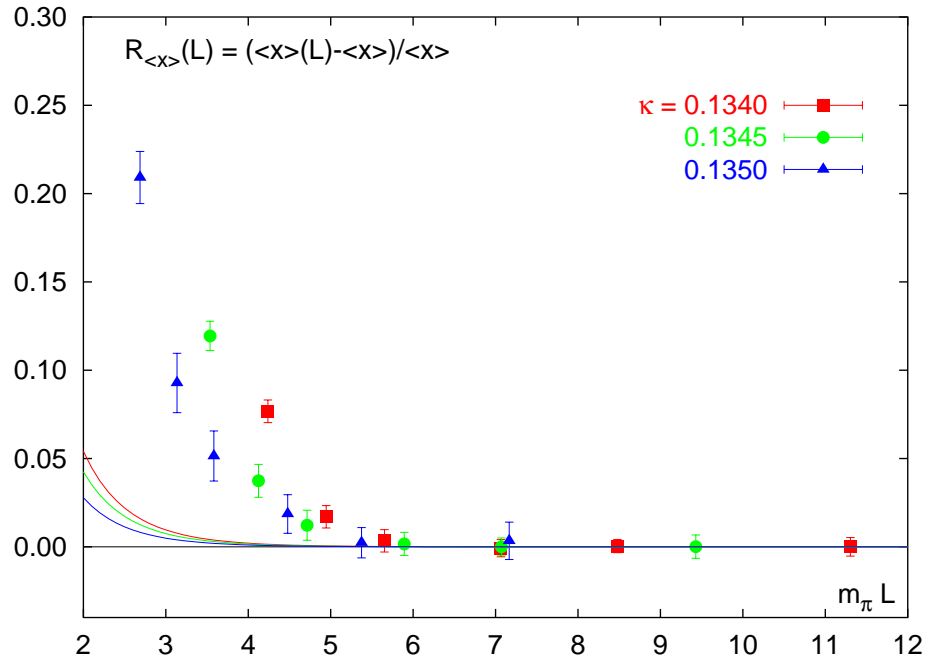


Figure 5: Finite size dependence of the twist-2 operator matrix element as a function of  $z = m_{\pi}L$ . The solid curves indicate the finite size effects of the pion mass described by formula (17) for comparison.

of chiral perturbation theory

$$\begin{aligned}
R_{m_\pi}(L) &\simeq \frac{3}{8\pi^2} \left(\frac{m_\pi}{F_\pi}\right)^2 \left[ \frac{K_1(m_\pi L)}{m_\pi L} + \frac{2 K_1(\sqrt{2} m_\pi L)}{\sqrt{2} m_\pi L} \right] \\
&\simeq \frac{3}{4(2\pi)^{3/2}} \left(\frac{m_\pi}{F_\pi}\right)^2 \left[ \frac{e^{-m_\pi L}}{(m_\pi L)^{3/2}} + \frac{2 e^{-\sqrt{2} m_\pi L}}{(\sqrt{2} m_\pi L)^{3/2}} \right], \quad (17)
\end{aligned}$$

where we have interpolated the results for  $m_\pi/F_\pi$  of ref. [18] to our  $\kappa$  values.

A possible explanation for this behaviour is the fact that the validity of the p-expansion of chiral perturbation theory, used to determine formula (17), is limited by the constraint  $F_\pi L \gg 1$ . For the lattice size  $L/a = 12$  we find instead  $F_\pi L \simeq 1$ .

The interesting (and worrisome) result is that while the FSE for the pion mass vanish for  $m_\pi L \geq 4$ , the FSE for  $\langle x \rangle$  vanish only for  $m_\pi L \geq 5.5$ . At  $m_\pi L \sim 4$  where the FSE for the pion mass are consistent with zero, the 3-point function, due to the FSE, is overestimated by around 5%.

## 4 Conclusions

As suggested in [7], the breaking of the gauge center symmetry  $Z_3$  can be responsible for larger FSE of the hadron masses in the unquenched case compared to the quenched case. This effect, that would lead to power law FSE, is dominant for intermediate volumes. It is also well known that FSE are larger for the nucleon mass than for the pion mass [7, 8], and moreover, the lattice size where the power law behavior disappears in favor of an exponential one is larger for the nucleon than for the pion. There is then a danger that the systematic uncertainty coming from FSE in the current unquenched determinations of the nucleon matrix elements is severely underestimated. At the moment there are no studies of FSE for 3-point functions involving twist-2 operators between nucleon states, and to our knowledge, this is the first study of FSE of matrix elements involving twist-2 operators.

We think, it would be important and urgent to have an analytical description of the FSE and in particular of the size dependence of the twist-2 matrix elements between hadron states, along the line of the computations performed in the framework of chiral perturbation theory, in [20] and [21].

## Acknowledgements

We thank S. Dürr, R. Sommer and S. Capitani for many useful discussions. The computer center at NIC/DESY Zeuthen provided the necessary technical help and the computer resources. This work was supported by the EU IHP Network on Hadron Phenomenology from Lattice QCD and by the DFG Sonderforschungsbereich/Transregio SFB/TR9-03.

## References

- [1] LHPC-SESAM coll.: D. Dolgov *et al.*, Phys. Rev. **D66** (2002) 034506.
- [2] QCDSF coll.: M. Göckeler *et al.*, Nucl. Phys. B (Proc. Suppl.) **119** (2003) 398.
- [3] ZeRo coll.: M. Guagnelli *et al.*, Nucl. Phys. **B664** (2003) 276.
- [4] ZeRo coll.: A. Shindler *et al.*, Nucl. Phys. B (Proc. Suppl.) **129** (2004) 278.
- [5] W. Detmold *et al.*, Phys. Rev. Lett. **87** (2001) 172001.
- [6] ZeRo coll.:I. Wetzorke *et al.*, Nucl. Phys. B (Proc. Suppl.) **129** (2004) 281.
- [7] S. Aoki *et al.*, Phys. Rev. **D50** (1994) 486.
- [8] B. Orth, T. Lippert and K. Schilling, Nucl. Phys. B (Proc. Suppl.) **129** (2004) 173.
- [9] QCDSF-UKQCD coll.: A. Ali Khan *et al.*, Nucl. Phys. **B689** (2004) 175.
- [10] M. Lüscher, R. Narayanan, P. Weisz and U. Wolff, Nucl. Phys. **B384** (1992) 168;  
S. Sint, Nucl. Phys. **B421** (1994) 135.
- [11] ALPHA coll.: M. Guagnelli *et al.*, Nucl. Phys. **B560** (1999) 465.
- [12] M. Lüscher, S. Sint, R. Sommer, P. Weisz, Nucl. Phys. **B478** (1996) 365.
- [13] ZeRo coll.: M. Guagnelli *et al.*, hep-lat/0405027.
- [14] B. Sheikholeslami, R. Wohlert, Nucl. Phys. **B259** (1985) 572;  
ALPHA coll.: M. Lüscher *et al.*, Nucl. Phys. **B491** (1997) 323.
- [15] R. Sommer, Nucl. Phys. **B411** (1994) 839.
- [16] M. Fukugita *et al.*, Phys. Lett. **B294** (1992) 380.
- [17] M. Lüscher, Commun. Math. Phys. **104** (1986) 177.
- [18] ALPHA coll.: J. Garden *et al.*, Nucl. Phys. **B571** (2000) 237.
- [19] J. Gasser and H. Leutwyler, Phys. Lett. **B184** (1987) 83.
- [20] G. Colangelo and S. Dürr, Eur.Phys.J. **C33** (2004) 543.
- [21] D. Becirevic and G. Villadoro, Phys. Rev. **D69** (2004) 054010.